

Seminar Report

Effect of Inclined Hole on a Plate of Finite Thickness

Naman Kothari

17BME049

Jheel Patel

17BME044

Guide

Prof. Vishal Mehta vishal.mehta@nirmauni.ac.in

Mechanical Engineering Department

Institute of Technology

Nirma University

Ahmedabad – 382 481

Certificate

This is to certify that Naman Kothari (Roll call 17BME044) and Jheel Patel (Roll call 17BME044) has successfully completed the seminar on

Date:

Guide: Prof. Vishal Mehta

H.O.D.:

Index

Title	Page No.
Acknowledgements	I
Abstract	II
List of figures/diagrams	III
List of tables	IV
List of graphs	V
Introduction	1
1. Mathematical Concepts	2
2. Derivation of stress functions for a straight hole (2-D case)	5
3. Plate dimensions, notation and load configuration	8
4. Analysis results	12
4.1.Circular Hole	
4.1.1. Uniaxial loading	
4.1.1.1.Variation in Z inclination	
4.1.1.2.Variation in Y Inclination	
4.1.1.3.Rotation in XY Plane with Z inclination of 30	
4.1.1.4.Variation in Hole Diameter (Z=30)	
4.1.1.5.Variation in Hole Diameter (Y=30)	
4.1.1.6.Contour Plot (Uniaxial Tension)	
4.1.2. Bending moment	
4.1.2.1.Variation in Y Inclination	
4.1.2.2.Variation in Z Inclination	
4.1.2.3.Rotation in XY Plane with Z inclination of 30	
4.2.Elliptic Hole	
4.2.1. Variation in axis length	
4.2.2. Variation in axis orientation	
Conclusion	29
References	30

Acknowledgements

We have taken efforts in this project. However, it would not have been possible without the kind support and help of many individuals and organizations. We would like to extend our sincere thanks to all of them. We are highly indebted to our guide Prof. Vishal Mehta for his guidance and constant supervision as well as for providing necessary information regarding the project & also for their support in completing the project.

We would like to express our gratitude towards our parents for their kind co-operation and encouragement which help us in completion of this project.

We would like to express our special gratitude and thanks to our mentor Prof. B. A. Shah for giving us such attention and time.

And many thanks and appreciations also go to our friends for their constructive criticism on the project and willingly helping us out with their abilities.

Naman Kothari, Jheel Patel

Abstract

The most important role of engineering is to obtain most economical and optimized solution to a problem. When it comes to mechanical designing the component must work properly within safety limits. It is important to evaluate the stress distributions in the component. Component must be designed such that stress raisers are minimized. In this study an alternate approach is used for evaluating stress distribution is a square plate under loading with inclined hole in the centre. Ansys FEA software is used for the numerical analysis. The results are compared with the theoretical values.

List of figures/diagrams

	Page No.
1. Stresses acting on the faces of an infinitesimal element into consideration	3
2. Plate under loading. -Timoshenko	5
3. Plate Dimensions	8
4. Configuration of Tensile Load	9
5. Configuration of Bending Moment	9
6. Elliptic Hole dimension	10
7. Hole axis orientation and notation	11
8. Von Mises stress contours for Uniaxial Loading ($\theta=30$ deg and $\phi=0$)	13
9. Von Mises stress contours for Uniaxial Loading ($\theta=30$ deg and $\phi=90$)	14
10. Contour plot for straight hole	18
11. Contour plot for $\theta=45$ and $\phi=90$ deg inclination	19
12. Contour plot for $\theta=45$ and $\phi=0$ deg. inclination	20
13. Von Mises stress contours ($\theta=30$ and $\phi=90$), Bending Moment	22
14. Von Mises stress contours ($\theta=30$ and $\phi=0$), Bending Moment	24
15. Elliptic Hole notations	25

List of tables

	Page No.
1. Stress concentration with hole inclination	12-13
2. Stress concentration with hole diameter	16
3. Maximum Von Mises with hole inclination (Bending Moment)	21
4. Stress concentration with hole axis dimensions and orientation	26

List of graphs

	Page No.
1. Variation of Maximum Von Mises stress wrt. change in θ angle (0-56 deg) at $\varphi=0$	13
2. Variation of Maximum Von Mises stress wrt. change in θ angle (56-60 deg) at $\varphi=0$	14
3. Variation of Maximum Von Mises stress wrt. change in θ angle at $\varphi=90$	15
4. Variation of Maximum Von Mises stress wrt. change in φ angle at $\theta=30$	15
5. Variation of Maximum Von Mises stress wrt. change in hole the diameter ($\theta=30$ and $\varphi=0$). Hole diameter is in mm	15
6. Variation of Maximum Von Mises stress wrt. Change in hole thickness ($\theta=30$ and $\varphi=90$). Hole diameter is in mm	17
7. Von Mises along the path shown by black line in Fig. 9 for straight hole	18
8. Von Mises along the path shown by black line in Fig. 10 for $\theta=45$ and $\varphi=90$ deg inclination	19
9. Von Mises along the path shown by black line in Fig. 11 for $\theta=45$ and $\varphi=0$ deg. inclination	20
10. Variation of Maximum Von Mises stress wrt. change in θ angle at $\varphi=90$	23
11. Variation of Maximum Von Mises stress wrt. change in θ angle at $\varphi=0$	25
12. Variation of Maximum Von Mises stress wrt. change in φ angle at $\theta=30$	25
13. Stress concentration vs. a axis variation	27
14. Stress concentration vs. b axis variation	27
15. Stress concentration vs. hole orientation (φ)	28

Introduction

Stress analysis forms the basic backbone for Engineering Design. Every mechanical component is designed based on the stress field produced in the component under loading or running condition. The design is optimised for weight reduction and at the same time the maximum stress produced shouldn't exceed the material limits. In many components the presence of notches and discontinuities (holes, etc.) are inevitable. For example, in mechanical fastening holes are to be made in the components. These discontinuities are sources of stress raisers. At the discontinuities the stresses are likely to increase many times more than the nominal values. Hence the design values considered have to be more than the nominal stress values. The factor by which the design values have to be increased is decided by the stress concentration factor (k_t), where

$$k_t = \frac{\text{maximum stress}}{\text{nominal stress}} = \frac{\sigma_{max}}{\sigma_{nom}} \quad 1$$

In this paper the effect of inclination and position of hole (in a plate of finite thickness under uniaxial tension and bending moment) on the stress concentration factor will be studied. From which better design criteria will be derived for safe design.

1 | Mathematical Concept

Before going into general theorems certain terms must be defined.

Stresses are denoted by stress tensor,

$$\boldsymbol{\sigma} = \begin{pmatrix} \sigma_{xx} & \sigma_{xy} & \sigma_{xz} \\ \sigma_{yx} & \sigma_{yy} & \sigma_{yz} \\ \sigma_{zx} & \sigma_{zy} & \sigma_{zz} \end{pmatrix} \quad 2$$

Because of symmetry conditions the above stress tensor must be symmetric,

$$\sigma_{ij} = \sigma_{ji}$$

And diagonal terms denote normal stresses along the direction denoted by the indices. And off diagonal terms denote the shear stresses with first index denotes the face and second index denotes the direction (Fig. 1).

The corresponding strain tensor is given by,

$$\boldsymbol{\varepsilon} = \begin{pmatrix} \varepsilon_{xx} & \varepsilon_{xy} & \varepsilon_{xz} \\ \varepsilon_{yx} & \varepsilon_{yy} & \varepsilon_{yz} \\ \varepsilon_{zx} & \varepsilon_{zy} & \varepsilon_{zz} \end{pmatrix} \quad 3$$

Under loading the component undergoes elastic deformation upto the yield point. Due to the deformation the points in the continuum are displaced. The strains produced at any point in the component volume can be derived from these displacements. Let the displacement of any point in the component volume be denoted by $\mathbf{u} = (u, v, w)$ vector for displacements in x, y and z directions respectively. The relation between the strains and displacements at any point are given by,

$$\begin{aligned} \varepsilon_{xx} &= \frac{\partial u}{\partial x}, \quad \varepsilon_{yy} = \frac{\partial v}{\partial y}, \quad \varepsilon_{zz} = \frac{\partial w}{\partial z} \\ \varepsilon_{xy} &= \frac{\partial u}{\partial y} + \frac{\partial v}{\partial x}, \quad \varepsilon_{xz} = \frac{\partial u}{\partial z} + \frac{\partial w}{\partial x}, \quad \varepsilon_{yz} = \frac{\partial v}{\partial z} + \frac{\partial w}{\partial y} \end{aligned} \quad 4$$

The stress field or stress distribution in a component is such that it must satisfy two laws⁴ viz. Compatibility equations and Equilibrium equations. Along with these two laws it must satisfy the boundary conditions. Hence compatibility equations, equilibrium equations and boundary conditions together decide the type of solution.

Equilibrium equations simply state that the summation of forces (produced due to stress distribution) acting on an infinitesimal element must be zero.

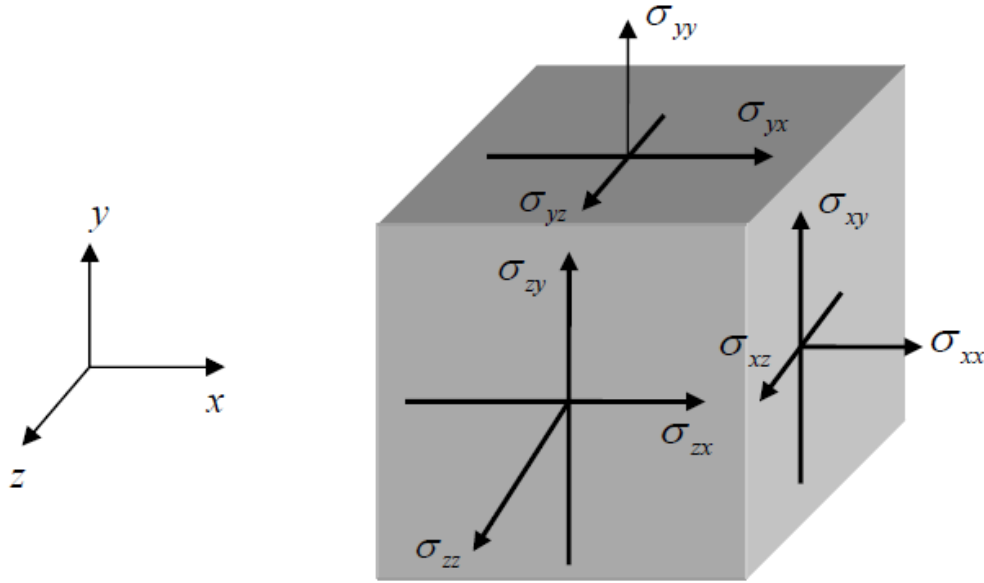


Fig 1. Stresses acting on the faces of an infinitesimal element into consideration (Equilibrium of Stress - Kelly, engineering.auckland.ac.nz)

Equilibrium condition when applied on the above infinitesimal element yields following three equilibrium equations.

$$\frac{\partial \sigma_{xx}}{\partial x} + \frac{\partial \sigma_{xy}}{\partial y} + \frac{\partial \sigma_{xz}}{\partial z} + X = 0$$

$$\frac{\partial \sigma_{yy}}{\partial y} + \frac{\partial \sigma_{xy}}{\partial x} + \frac{\partial \sigma_{yz}}{\partial z} + Y = 0$$

$$\frac{\partial \sigma_{zz}}{\partial z} + \frac{\partial \sigma_{xz}}{\partial x} + \frac{\partial \sigma_{yz}}{\partial y} + Z = 0$$

5

Where X, Y and Z are body forces (gravity, electromagnetic).

Equilibrium equations (2) must be satisfied at all points throughout the component volume.

From equations 4 it is evident that the strains are related in a specific way and random strain distribution is not possible. The strains must be such that they are compatible with each other. From equations 4 following equations can be derived,

$$\begin{aligned}
\frac{\partial^2 \varepsilon_{xx}}{\partial z^2} + \frac{\partial^2 \varepsilon_{zz}}{\partial y^2} &= 2 \frac{\partial^2 \varepsilon_{yz}}{\partial y \partial z}, & \frac{\partial^2 \varepsilon_{xx}}{\partial y \partial z} &= \frac{\partial}{\partial x} \left(-\frac{\partial \varepsilon_{yz}}{\partial x} + \frac{\partial \varepsilon_{zx}}{\partial y} + \frac{\partial \varepsilon_{xy}}{\partial z} \right) \\
\frac{\partial^2 \varepsilon_{zz}}{\partial x^2} + \frac{\partial^2 \varepsilon_{xx}}{\partial z^2} &= 2 \frac{\partial^2 \varepsilon_{zx}}{\partial z \partial x}, & \frac{\partial^2 \varepsilon_{yy}}{\partial z \partial x} &= \frac{\partial}{\partial y} \left(+\frac{\partial \varepsilon_{yz}}{\partial x} - \frac{\partial \varepsilon_{zx}}{\partial y} + \frac{\partial \varepsilon_{xy}}{\partial z} \right) \\
\frac{\partial^2 \varepsilon_{xx}}{\partial y^2} + \frac{\partial^2 \varepsilon_{yy}}{\partial x^2} &= 2 \frac{\partial^2 \varepsilon_{xy}}{\partial x \partial y}, & \frac{\partial^2 \varepsilon_{zz}}{\partial x \partial y} &= \frac{\partial}{\partial z} \left(+\frac{\partial \varepsilon_{yz}}{\partial x} + \frac{\partial \varepsilon_{zx}}{\partial y} - \frac{\partial \varepsilon_{xy}}{\partial z} \right)
\end{aligned} \tag{6}$$

Above equations can be transformed into relations between components of stress using Hooke's law, giving following equations,

$$\begin{aligned}
(1 + \nu) \nabla^2 \sigma_{xx} + \frac{\partial^2 \theta}{\partial x^2} &= 0, & (1 + \nu) \nabla^2 \sigma_{yz} + \frac{\partial^2 \theta}{\partial y \partial z} &= 0 \\
(1 + \nu) \nabla^2 \sigma_{yy} + \frac{\partial^2 \theta}{\partial y^2} &= 0, & (1 + \nu) \nabla^2 \sigma_{xz} + \frac{\partial^2 \theta}{\partial x \partial z} &= 0 \\
(1 + \nu) \nabla^2 \sigma_{zz} + \frac{\partial^2 \theta}{\partial z^2} &= 0, & (1 + \nu) \nabla^2 \sigma_{xy} + \frac{\partial^2 \theta}{\partial x \partial y} &= 0
\end{aligned} \tag{7}$$

Equations of equilibrium and compatibility along with the boundary conditions must be solved in order to get the solutions for given system. For 2-D problems it is possible to obtain approximate and sometimes exact solutions by assuming proper stress functions (Airy stress functions). But for 3-D problem, solutions are available for simple and special cases only.

But approximate solutions can be obtained from numerical methods. Here Finite Element Method will be used to obtain graphical solutions.

Static structural analysis was carried out in Ansys mechanical APDL.

2 | Derivation of stress functions for a straight hole (2-D case)

For an infinitely wide plate with circular hole with radius a at the centre, the stress distribution near the hole can be given by following equations in polar coordinates.

$$\begin{aligned}\sigma_r &= \frac{\sigma}{2} \left(1 + \frac{a^2}{r^2} \right) + \frac{\sigma}{2} \left(1 + 3 \frac{a^4}{r^4} - 4 \frac{a^2}{r^2} \right) \cos 2\theta \\ \sigma_\theta &= \frac{\sigma}{2} \left(1 + \frac{a^2}{r^2} \right) - \frac{\sigma}{2} \left(1 + 3 \frac{a^4}{r^4} \right) \cos 2\theta \\ \tau &= -\frac{\sigma}{2} \left(1 - 3 \frac{a^4}{r^4} + 2 \frac{a^2}{r^2} \right) \sin 2\theta\end{aligned}\tag{8}$$

Note: Here θ refers to the polar coordinate component and not the hole inclination angle.

At $\theta = \frac{\pi}{2}$, $r = a$,

$$\sigma_\theta = 3\sigma = \sigma_{max}\tag{9}$$

Its derivation is given below,

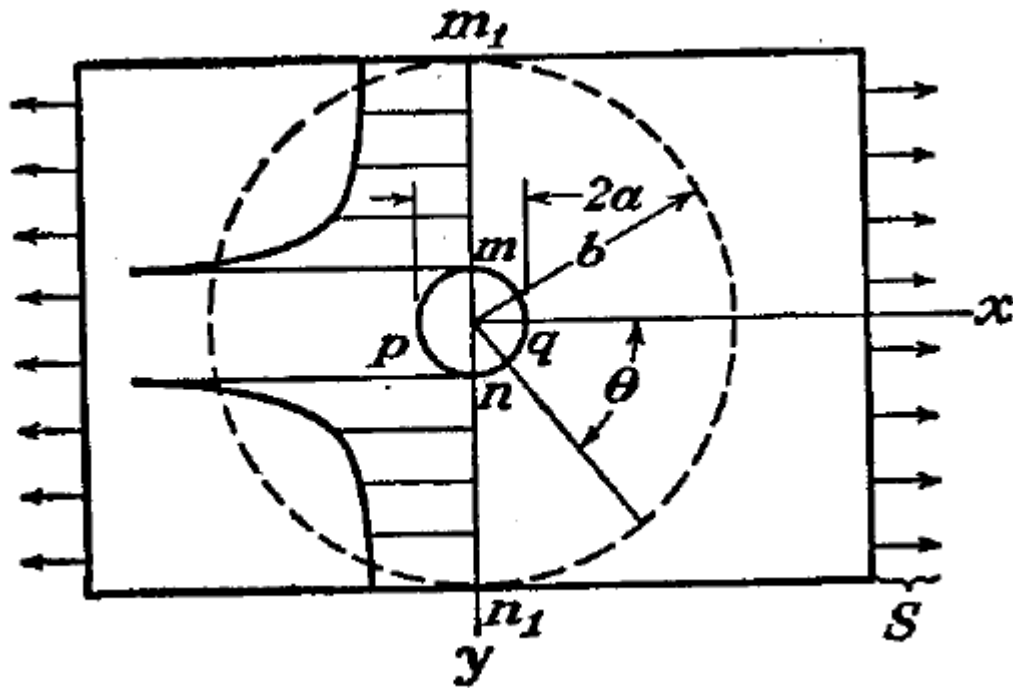


Fig. 2. Plate under loading. -Timoshenko

Consider a plate under uniaxial tension in x-direction as shown in the figure. In case of a small circular hole in the middle of the plate the stress distribution will change around the hole but at distances more than the radius of the hole the stresses will be uniform (Saint-Venant's principle).

In region $r = b$ the stresses will be same as in the case of plate without a hole, which is given by,

$$(\sigma_r)_{r=b} = S \cos^2 \theta = \frac{1}{2} S (1 + \cos 2\theta)$$

$$(\tau_{r\theta})_{r=b} = -\frac{1}{2} S \sin 2\theta$$
10

Stress distribution inside the ring (with inner and outer radii a and b respectively) is dictated by the stress outside the ring given by above equations. The stress distribution inside the ring consists of two parts:

1. Due to the constant component $\frac{1}{2}S$ of the normal forces which can be calculated using following equations for symmetrical stress distribution about an axis,

$$\sigma_r = \frac{a^2 b^2 (p_o - p_i)}{b^2 - a^2} \cdot \frac{1}{r^2} + \frac{p_i a^2 - p_o b^2}{b^2 - a^2}$$

$$\sigma_\theta = -\frac{a^2 b^2 (p_o - p_i)}{b^2 - a^2} \cdot \frac{1}{r^2} + \frac{p_i a^2 - p_o b^2}{b^2 - a^2}$$
11

Where, p_i and p_o are the uniform internal and external pressures on a cylinder with inner and outer radii a and b respectively.

Which gives following stress distribution due constant stress component $\frac{1}{2}S$,

$$\sigma_r = \frac{S}{2} \left(1 - \frac{a^2}{r^2} \right)$$

$$\sigma_\theta = \frac{S}{2} \left(1 + \frac{a^2}{r^2} \right)$$
11

2. Stresses produced due to the normal forces $\frac{1}{2}S \cos 2\theta$ along with the shearing forces $-\frac{1}{2}S \sin 2\theta$ which can be derived from a stress function of the form

$$\varphi = f(r) \cos 2\theta$$
12

Substituting above equation in the compatibility equation,

$$\left(\frac{\partial^2}{\partial r^2} + \frac{1}{r} \frac{\partial}{\partial r} + \frac{1}{r^2} \frac{\partial^2}{\partial \theta^2} \right) \left(\frac{\partial^2 \varphi}{\partial r^2} + \frac{1}{r} \frac{\partial \varphi}{\partial r} + \frac{1}{r^2} \frac{\partial^2 \varphi}{\partial \theta^2} \right) = 0$$
13

Following ordinary differential equation is obtained,

$$\left(\frac{d^2}{dr^2} + \frac{1}{r} \frac{d}{dr} - \frac{4}{r^2}\right) \left(\frac{d^2 f}{dr^2} + \frac{1}{r} \frac{df}{dr} - \frac{4f}{r^2}\right) = 0 \quad 14$$

The general solution is

$$f(r) = Ar^2 + Br^4 + C \frac{1}{r^2} + D$$

Hence,

$$\varphi = \left(Ar^2 + Br^4 + C \frac{1}{r^2} + D\right) \cos 2\theta \quad 15$$

and stress components can be derived from stress function (eq. 15) using following equations,

$$\begin{aligned} \sigma_r &= \frac{1}{r} \frac{\partial \varphi}{\partial r} + \frac{1}{r^2} \frac{\partial^2 \varphi}{\partial \theta^2} = -\left(2A + \frac{6C}{r^4} + \frac{4D}{r^2}\right) \cos 2\theta \\ \sigma_\theta &= \frac{\partial^2 \varphi}{\partial r^2} = \left(2A + 12Br^2 + \frac{6C}{r^4}\right) \cos 2\theta \\ \tau_{r\theta} &= -\frac{\partial}{\partial r} \left(\frac{1}{r} \frac{\partial \varphi}{\partial \theta}\right) = \left(2A + 6Br^2 - \frac{6C}{r^4} - \frac{2D}{r^2}\right) \sin 2\theta \end{aligned} \quad 16$$

By applying the boundary conditions constants can be determined,

$$A = -\frac{S}{4}, \quad B = 0, \quad C = -\frac{a^4}{4}S, \quad D = \frac{a^2}{2}S$$

Substituting above constants in eqs. 16 and adding the results (eqs. 11) obtained in 1st part following stress distribution equations can be obtained,

$$\begin{aligned} \sigma_r &= \frac{S}{2} \left(1 - \frac{a^2}{r^2}\right) + \frac{S}{2} \left(1 + \frac{3a^4}{r^4} - \frac{4a^2}{r^2}\right) \cos 2\theta \\ \sigma_\theta &= \frac{S}{2} \left(1 + \frac{a^2}{r^2}\right) - \frac{S}{2} \left(1 + \frac{3a^4}{r^4}\right) \cos 2\theta \\ \tau_{r\theta} &= -\frac{S}{2} \left(1 - \frac{3a^4}{r^4} + \frac{2a^2}{r^2}\right) \sin 2\theta \end{aligned} \quad 17$$

3 | Plate Dimensions, Notation and Load Configuration

Circular Hole

Plate with following dimensions was selected:

Length	200 mm
Breadth	200 mm
Height	10 mm
Hole Diameter	20 mm
Load	5 MPa (on face normal to X-axis)

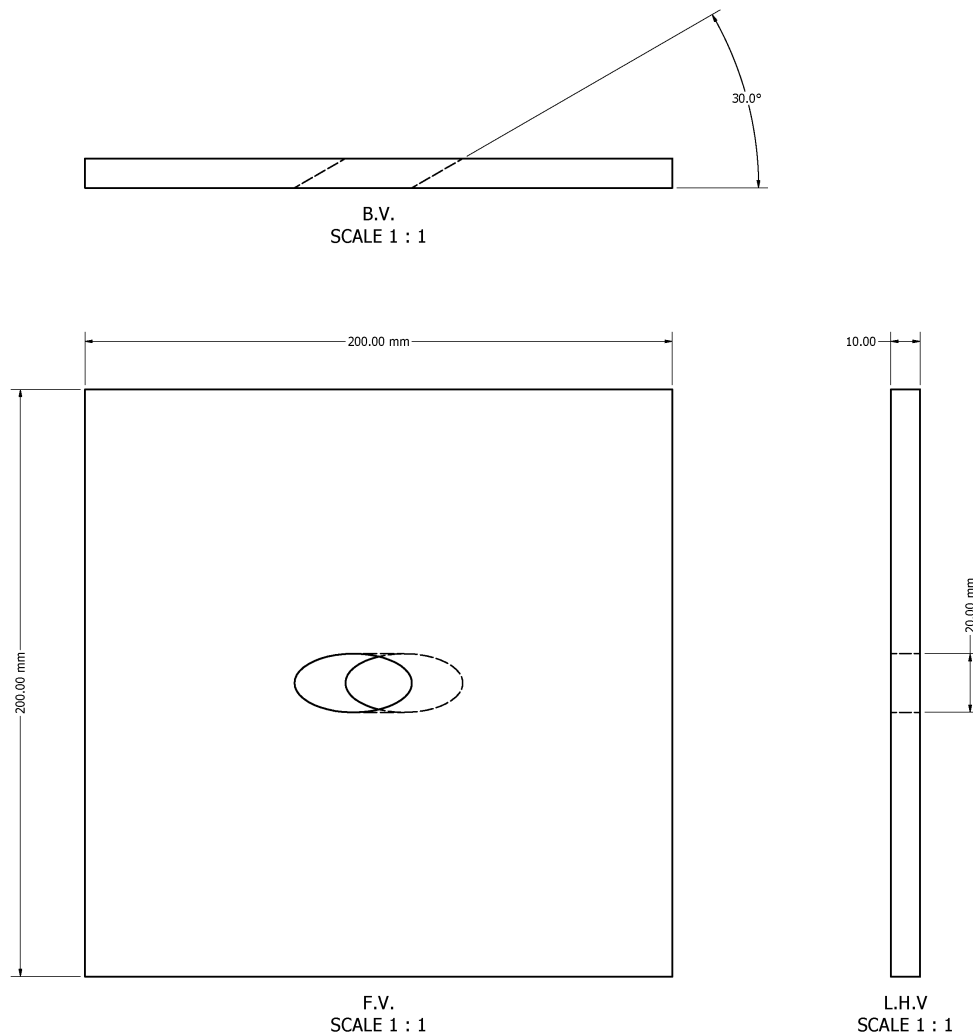


Fig. 3. Plate Dimensions

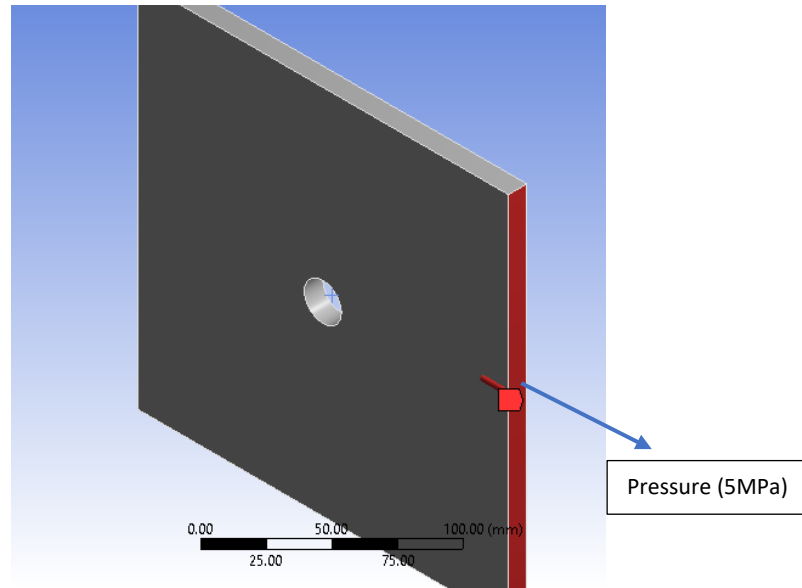


Fig. 4. Configuration of Tensile Load

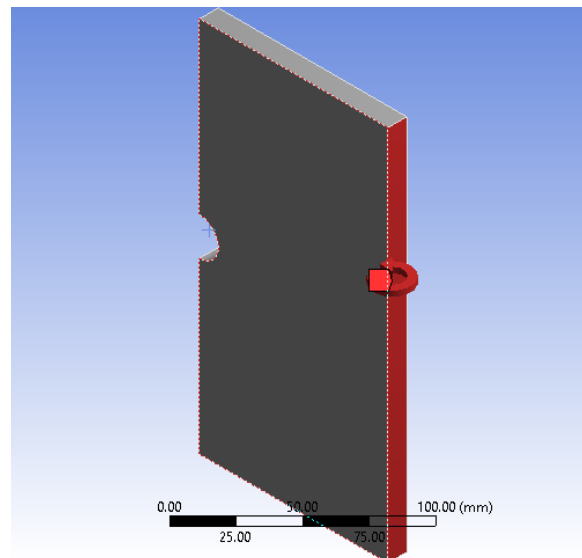


Fig. 5. Configuration of Bending Moment

Elliptic Hole

Plate with following dimensions was selected:

Length	200 mm
Breadth	200 mm
Height	10 mm
Load	1 MPa (on face normal to X-axis)

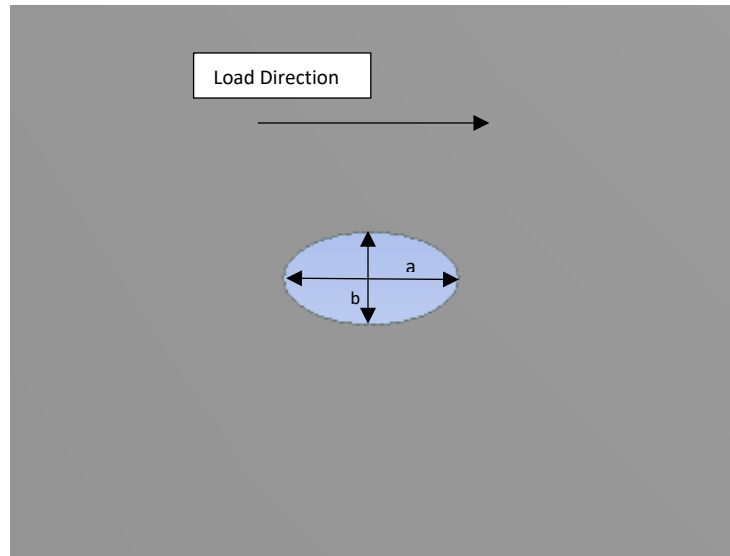


Fig. 6. Elliptic Hole dimension

Notations

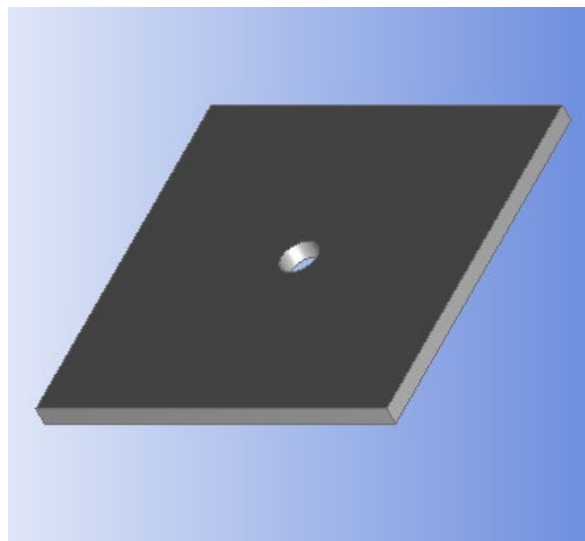
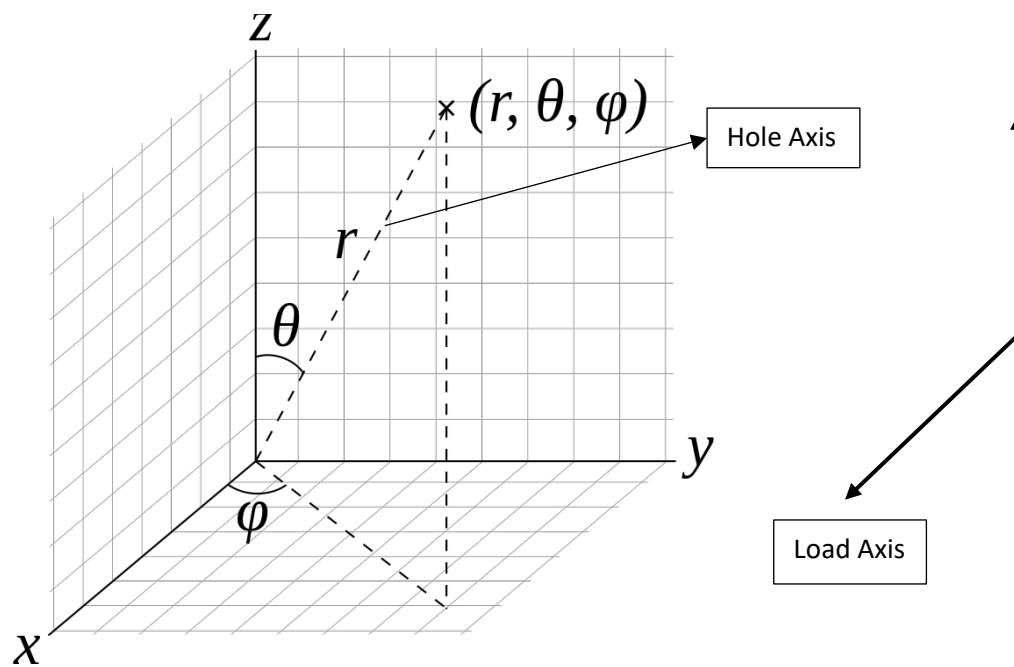


Fig. 7. Hole axis orientation and notation

4 | Analysis Results

4.1. Circular Hole

Circular hole is taken and analysis is carried out.

4.1.1. Uniaxial Tension

The plate is under uniaxial tension along X-axis.

θ ($\varphi=90$) in degrees	Stress Concentration
0	3.15556
2	3.15018
4	3.15056
6	3.15614
8	3.17134
10	3.21564
12	3.23272
14	3.2734
16	3.30264
18	3.32834
20	3.38506
22	3.47464
24	3.50214
26	3.57434
28	3.61054
30	3.74888
32	3.79014
34	3.93606
36	4.06786
38	4.19424
40	4.30754
42	4.40972
44	4.61258
46	4.76552
48	4.99716
50	5.19388
52	5.43258
54	5.72456

θ ($\varphi=0$) in degrees	Stress Concentration
0	3.15556
2	3.1351
4	3.10784
6	3.12626
8	3.1017
10	3.08732
12	3.09524
14	3.0695
16	3.0407
18	3.03064
20	2.99866
22	2.98342
24	2.92038
26	2.92572
28	2.87588
30	2.8432
32	2.818
34	2.77246
36	2.73656
38	2.6793
40	2.65054
42	2.6239
44	2.57254
46	2.53022
48	2.50852
50	2.45066
52	2.40854
54	2.35354

φ ($\theta=30$) in degrees	Stress Concentration
0	2.8432
3	2.8661
6	2.87644
9	2.89636
12	2.9222
15	2.9558
18	2.99006
21	3.01122
24	3.08796
27	3.12076
30	3.1694
33	3.1768
36	3.2464
39	3.31148
42	3.3555
45	3.37816
48	3.37084
51	3.46924
54	3.51862
57	3.55562
60	3.56966
63	3.55872
66	3.63434
69	3.69346
72	3.69598
75	3.7331
78	3.70796
81	3.70568

56	6.0714
58	6.43306
60	6.9911

56	2.29562
58	2.34556
60	2.4617

84	3.78816
87	3.80844
90	3.82288

Table 1. Stress concentration with hole inclination

4.1.1.1. Variation in θ ($\varphi = 0$)

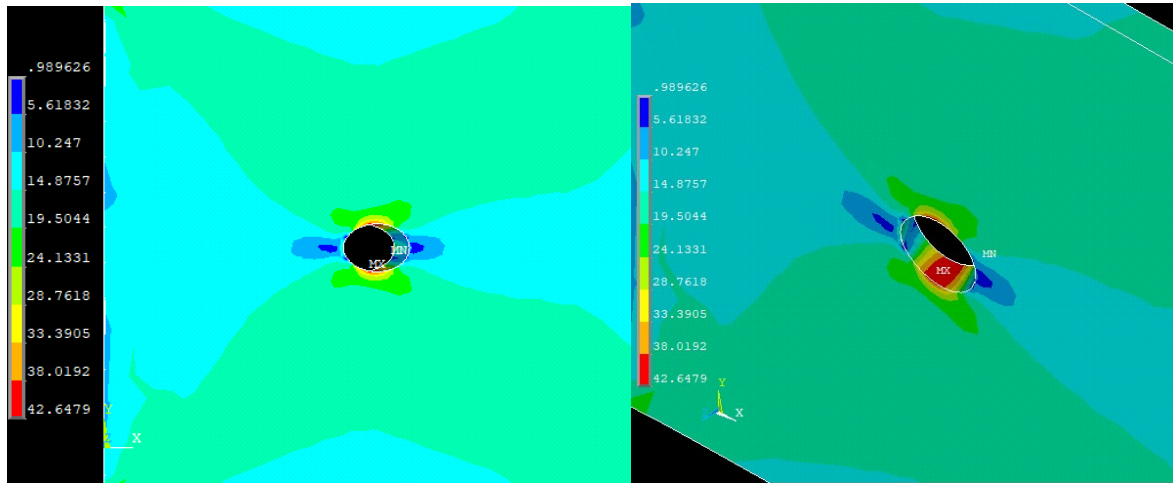
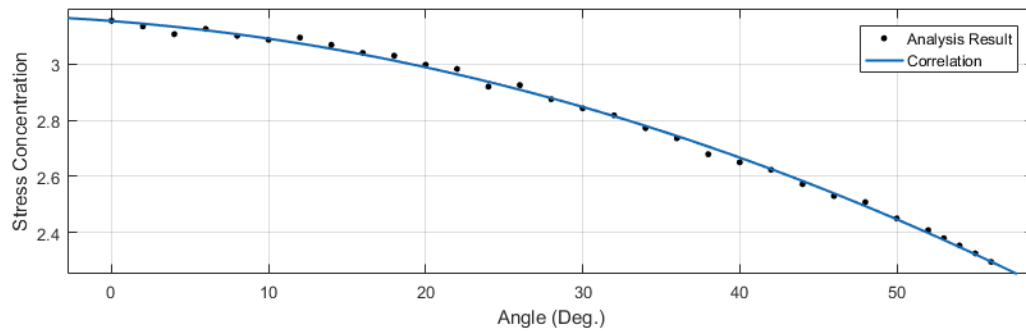
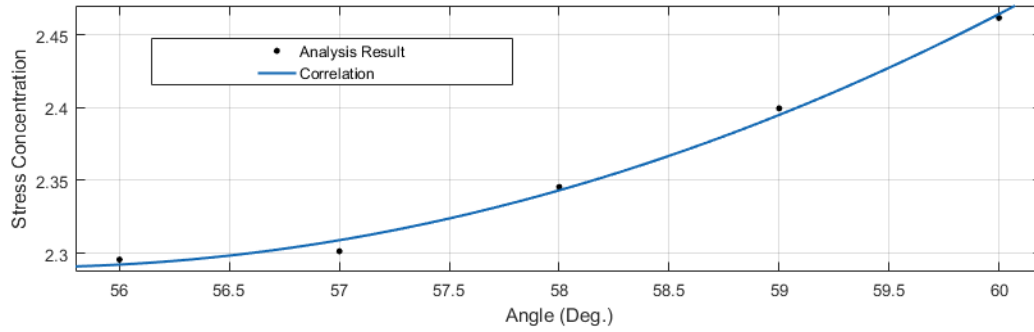


Fig. 8. Von Mises stress contours for Uniaxial Loading ($\theta=30$ deg and $\varphi=0$)



Plot 1. Variation of Maximum Von Mises stress wrt. change in θ angle (0-56 deg) at $\varphi=0$



Plot 2. Variation of Maximum Von Mises stress wrt. change in θ angle (56-60 deg) at $\phi=0$

From the above data it can be concluded that as the hole inclination increases w.r.t. **Z-axis (in ZX Plane)** the stress concentration decreases from 3.16 at 0 deg to 2.29 at 56 deg. After 56 deg stress concentration again starts to increase.

4.1.1.2. Variation in θ ($\phi = 90$)

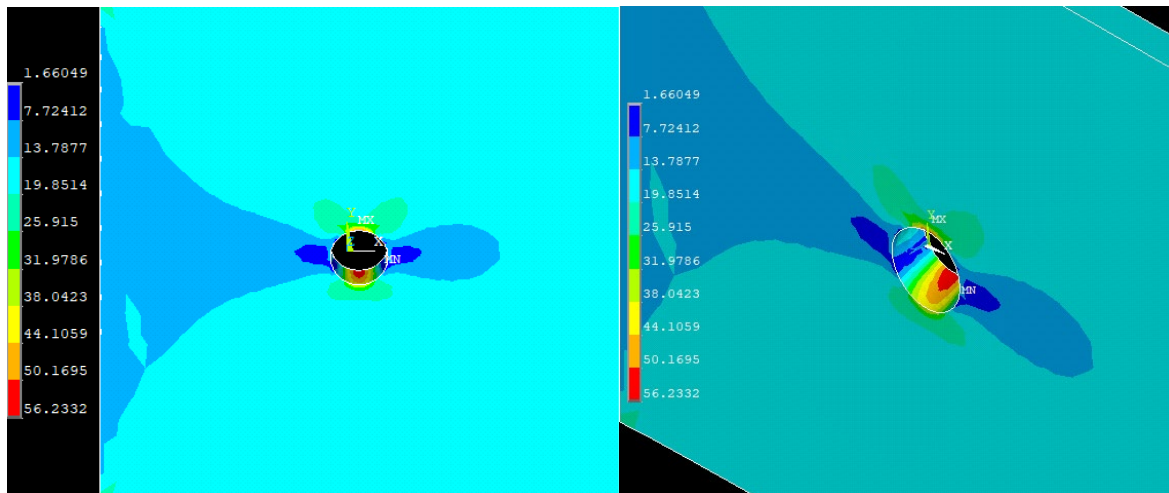
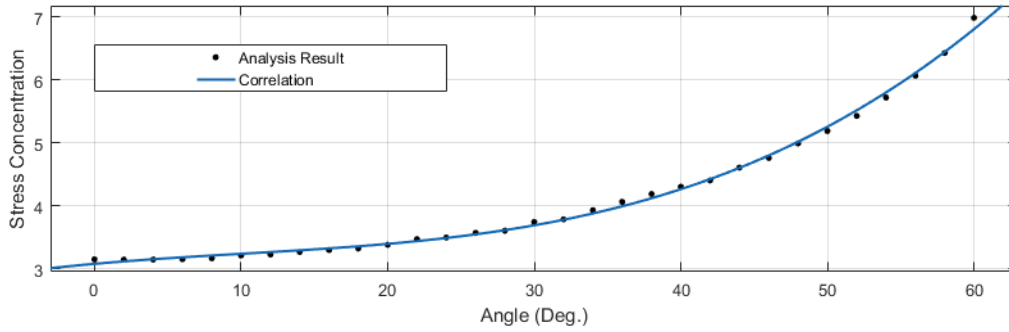


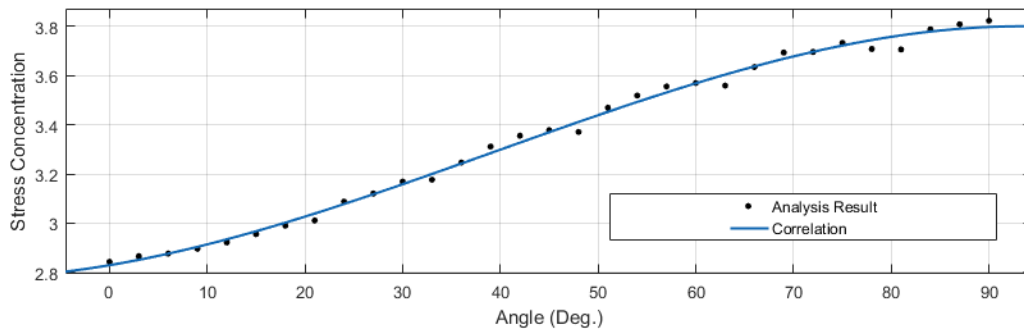
Fig. 9. Von Mises stress contours for Uniaxial Loading ($\theta=30$ deg and $\phi=90$)



Plot 3. Variation of Maximum Von Mises stress wrt. change in θ angle at $\phi=90$

From above data it can be concluded that as the hole inclination increases w.r.t. **Z-axis (in YZ Plane)** the Maximum Von Mises stress increases.

4.1.1.3. Rotation in XY Plane with Z inclination of 30



Plot 4. Variation of Maximum Von Mises stress wrt. change in ϕ angle at $\theta=30$

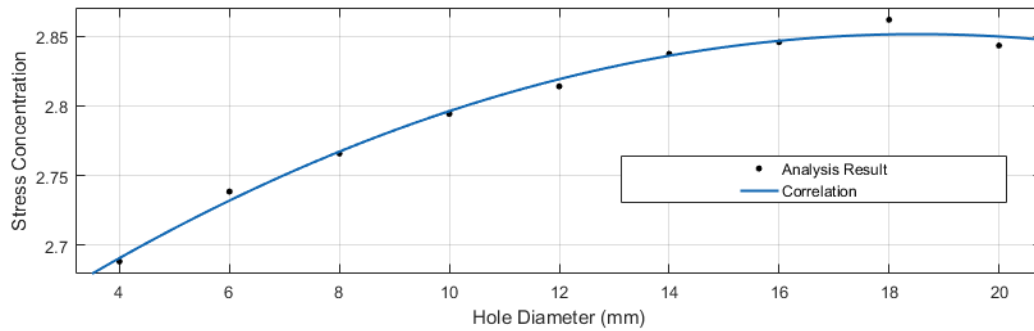
From above data it can be concluded that as hole swivels from load axis towards axis perpendicular to the load axis the Maximum Von Mises stress increases.

4.1.1.4. Variation in Hole Diameter ($\theta = 30$ and $\varphi = 0$)

HOLE_DIAMETER ($\theta=30, \varphi=90$)	Stress Concentration
20	3.74888
18	3.71396
16	3.754
14	3.69966
12	3.74722
10	3.76238
8	3.7055
6	3.6875
4	3.63792

HOLE_DIAMETER ($\theta=30, \varphi=90$)	Stress Concentration
20	2.8432
18	2.86164
16	2.8456
14	2.83718
12	2.81398
10	2.79424
8	2.76588
6	2.73854
4	2.68844

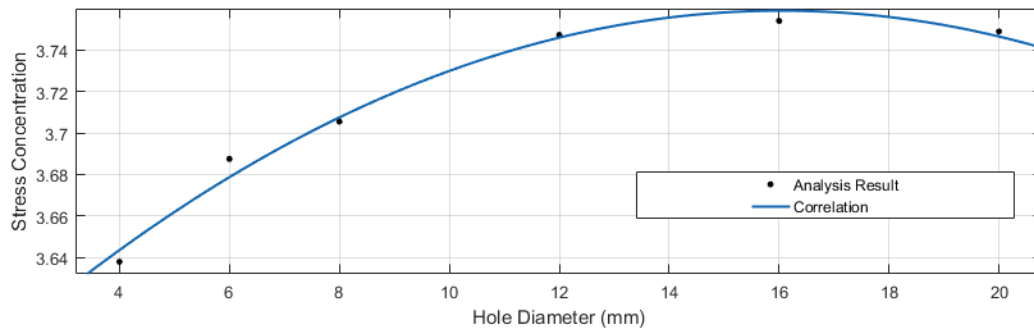
Table 2. Stress concentration with hole diameter



Plot 5. Variation of Maximum Von Mises stress wrt. change in hole the diameter ($\theta=30$ and $\varphi=0$). Hole diameter is in mm

From the above data it can be concluded that as the hole diameter increases from 4 mm to 20 mm the Maximum Von-Mises stress increases.

4.1.1.5. Variation in Hole Diameter ($\theta = 30$ and $\phi = 90$)



Plot 6. Variation of Maximum Von Mises stress wrt. Change in hole thickness ($\theta=30$ and $\phi=90$). Hole diameter is in mm

From the above data it can be concluded that as the Hole diameter increases from 4 mm to 20 mm the Maximum Von Mises stress remains nearly constant.

4.1.1.6. Contour Plot (Uniaxial Tension)

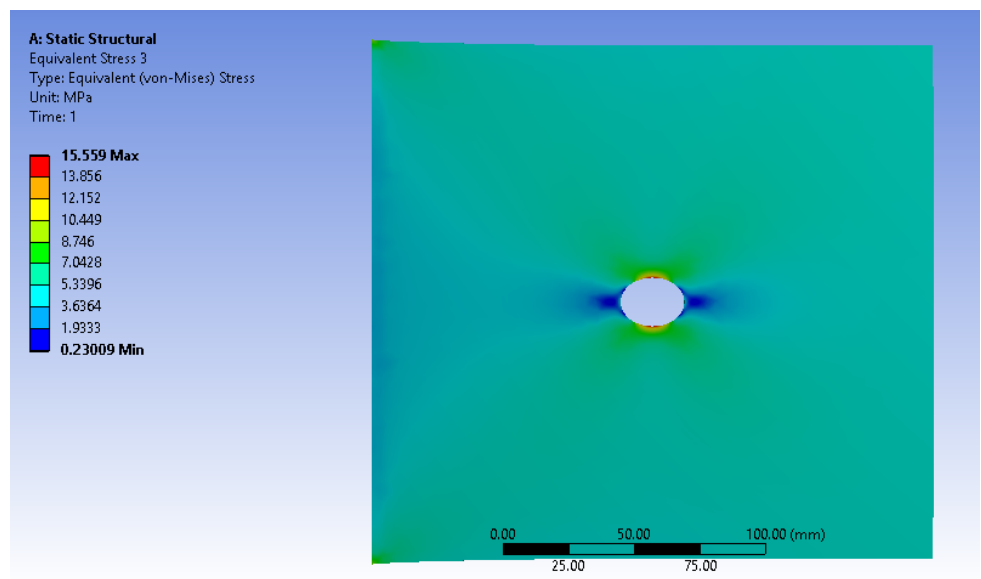
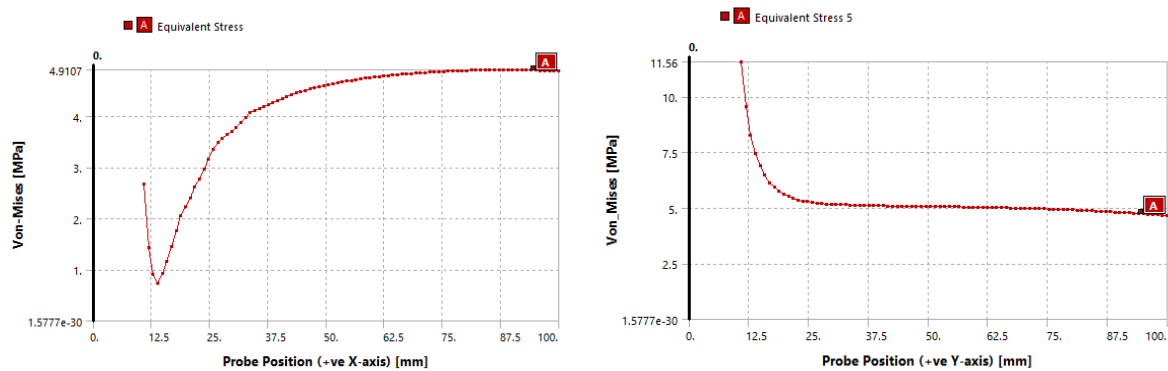


Fig. 10. Contour plot for straight hole



Plot 7. Von Mises along the path shown by black line in Fig. 9 for straight hole

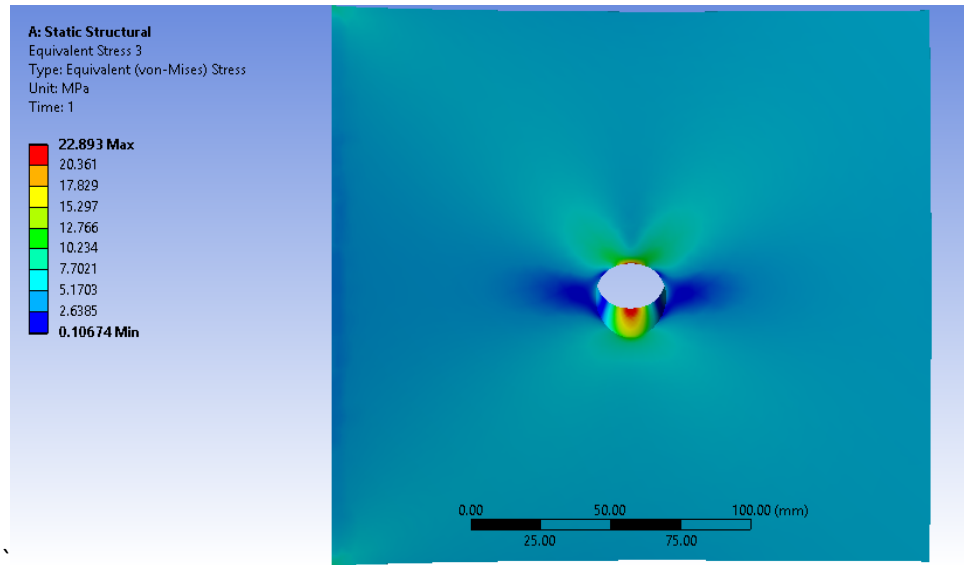
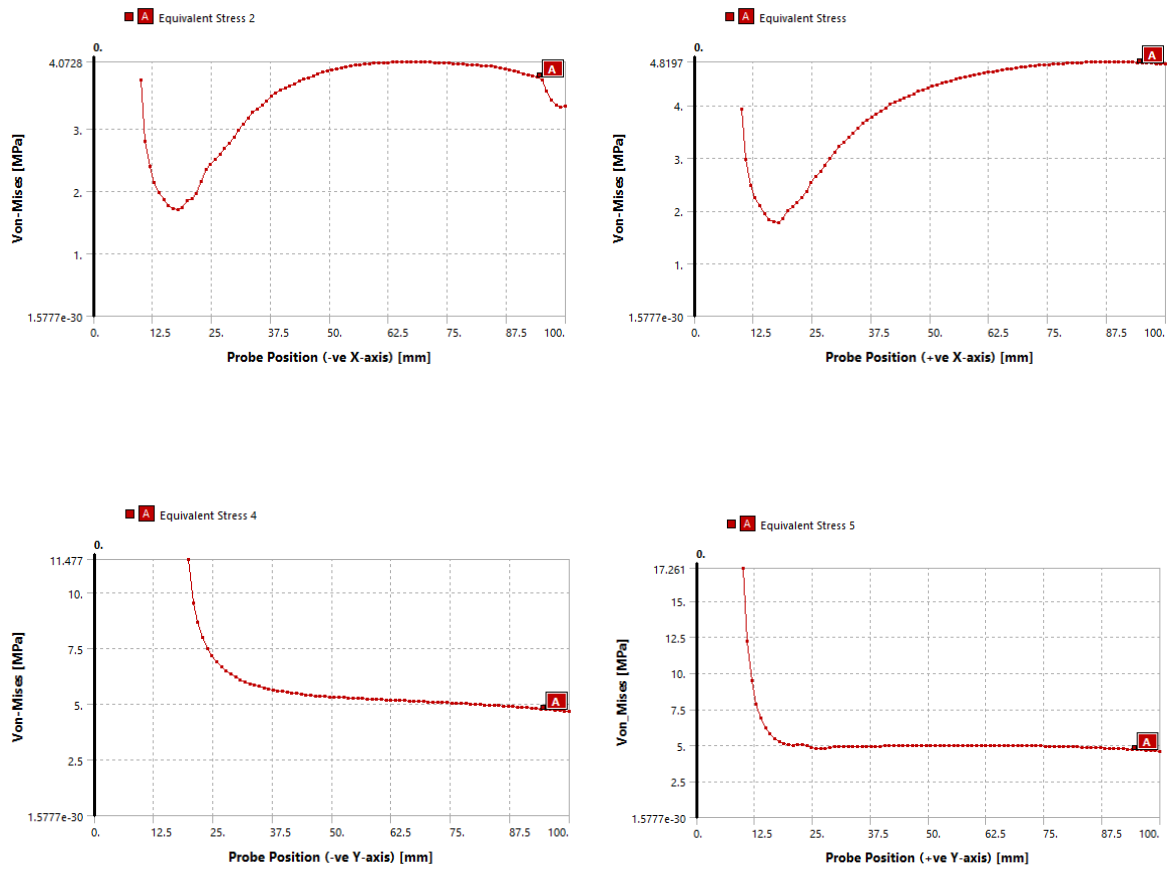


Fig. 11. Contour plot for $\theta=45$ and $\varphi=90$ deg inclination



Plot 8. Von Mises along the path shown by black line in Fig. 10 for $\theta=45$ and $\varphi=90$ deg inclination

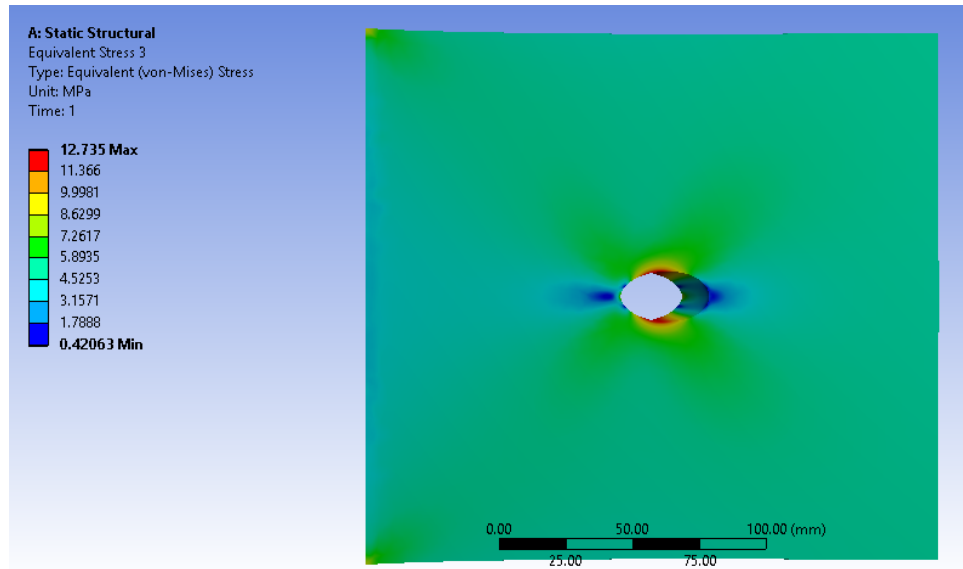
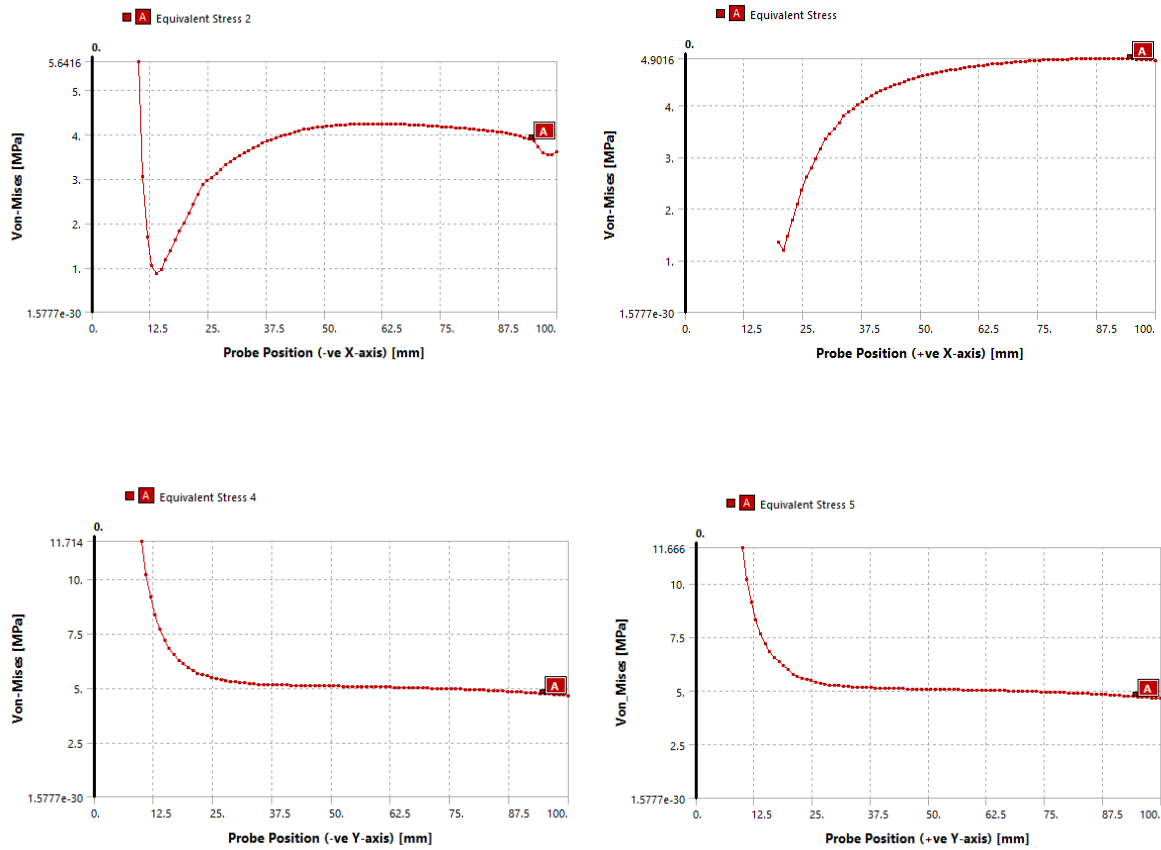


Fig. 12. Contour plot for $\theta=45$ and $\varphi=0$ deg. inclination



Plot 9. Von Mises along the path shown by black line in Fig. 11 for $\theta=45$ and $\varphi=0$ deg. inclination

4.1.2. Bending Moment

θ ($\varphi=90$) in degrees	Maximum Von-Mises	θ ($\varphi=0$) in degrees	Maximum Von-Mises	φ ($\theta=-30$) in degrees	Maximum Von-Mises
-60	128.144	-60	55.5898	0	56.5502
-55	110.487	-55	55.4745	5	56.1438
-50	97.4806	-50	55.722	10	56.5268
-45	88.5812	-45	55.4394	15	57.8197
-40	82.0264	-40	57.0846	20	58.8898
-35	76.4555	-35	55.8396	25	59.6411
-30	71.6985	-30	56.5502	30	61.6865
-25	68.5966	-25	56.8649	35	63.0452
-20	65.6276	-20	57.603	40	64.0073
-15	63.5589	-15	58.597	45	65.5791
-10	62.2216	-10	59.1971	50	67.0214
-5	60.9418	-5	59.7346	55	67.5208
0	59.8148	0	59.8148	60	69.1541
5	60.6342	5	59.6243	65	70.1672
10	62.4103	10	59.5158	70	70.6979
15	64.2282	15	58.4747	75	71.0574
20	65.5969	20	57.7151	80	71.7809
25	68.7865	25	56.7689	85	72.7183
30	71.9076	30	56.4988	90	72.0469
35	75.7497	35	56.0723		
40	82.007	40	55.6764		
45	88.6681	45	56.9054		
50	97.0672	50	54.9464		
55	110.321	55	56.6557		
60	126.671	60	55.9571		

Table 3. Maximum Von Mises with hole inclination

4.1.2.1. Variation in Y Inclination

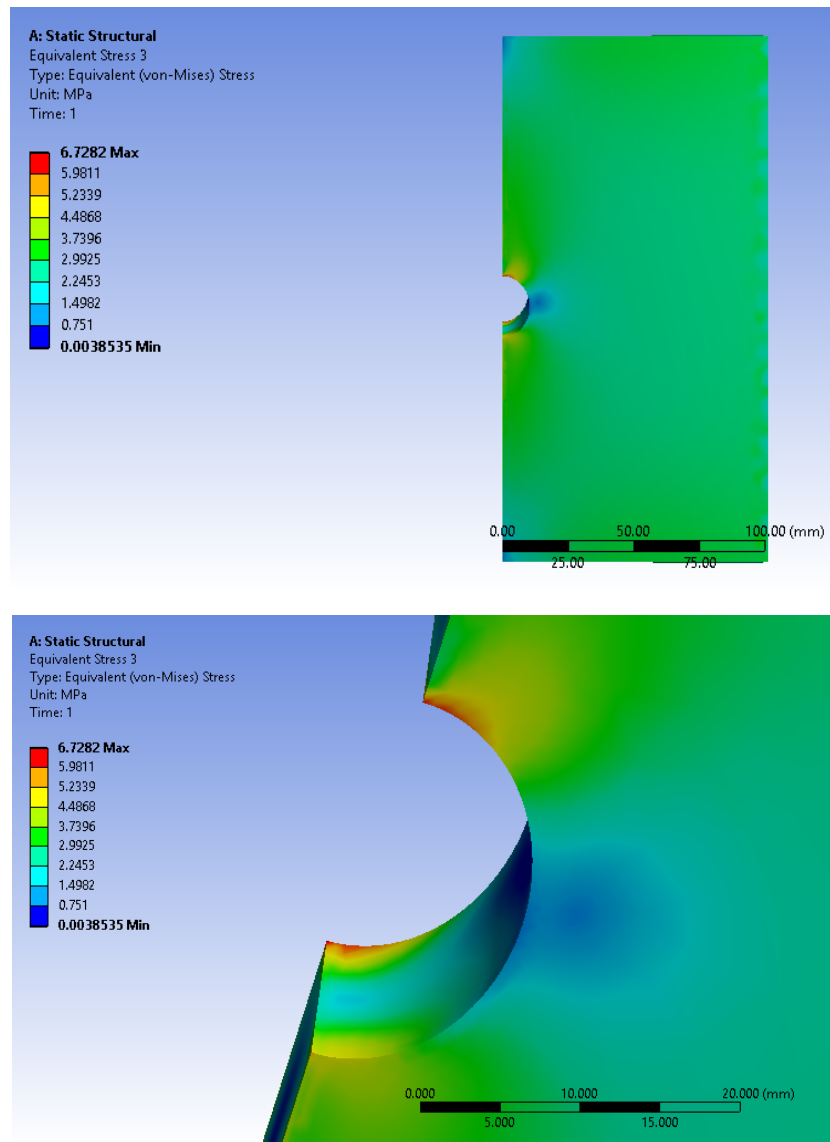
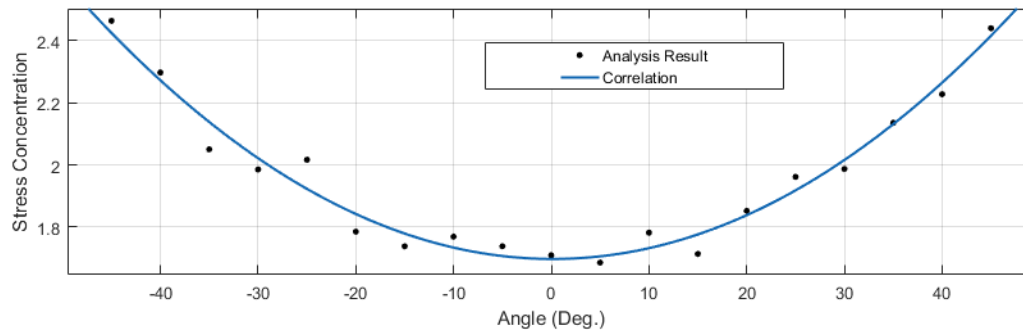


Fig. 13. Von Mises stress contours ($\theta=30$ and $\varphi=90$), Bending Moment



Plot 10. Variation of Maximum Von Mises stress wrt. change in θ anngle at $\varphi=90$

From the above data it can be concluded that as the inclination of hole wrt. **Z-axis (in YZ Plane)** increases the Maximum Von Mises stress also increases. For upto 25 deg the variation is linear and then its rate increases.

4.1.2.2. Variation in Z Inclination

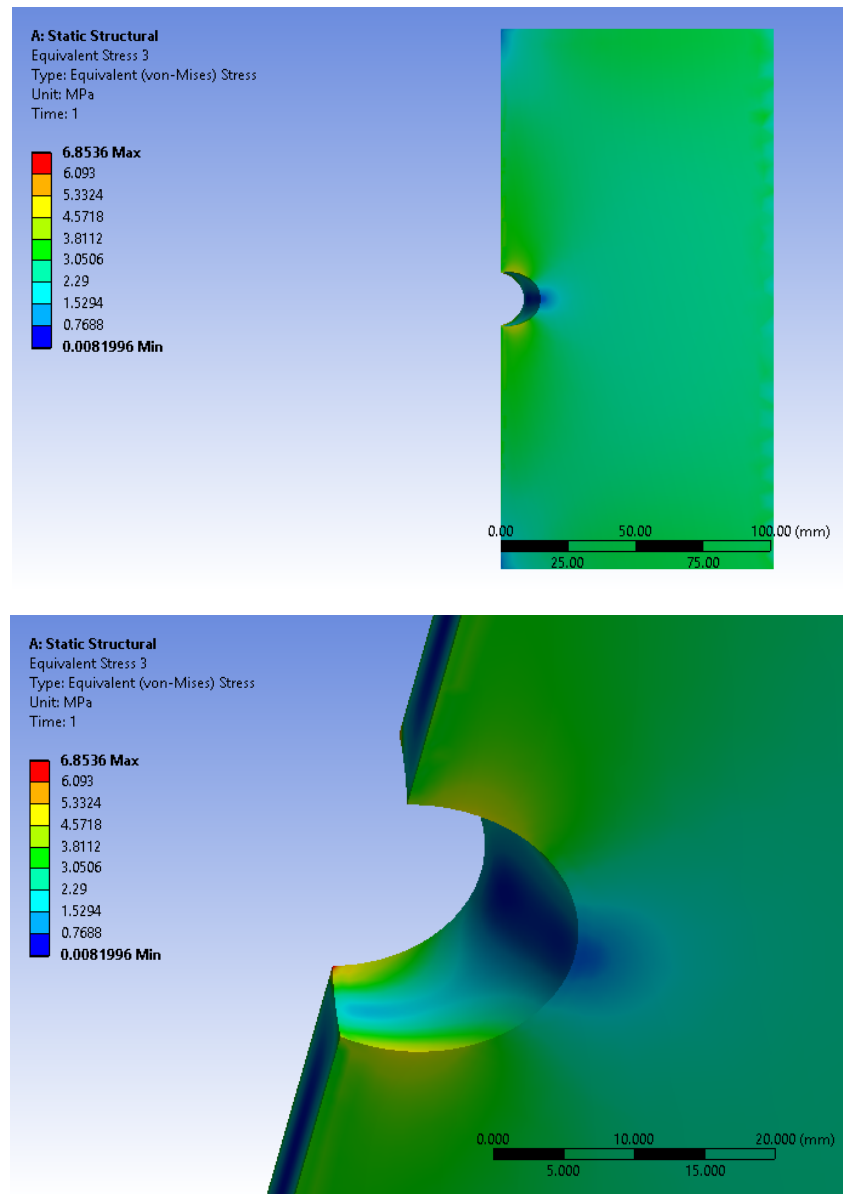
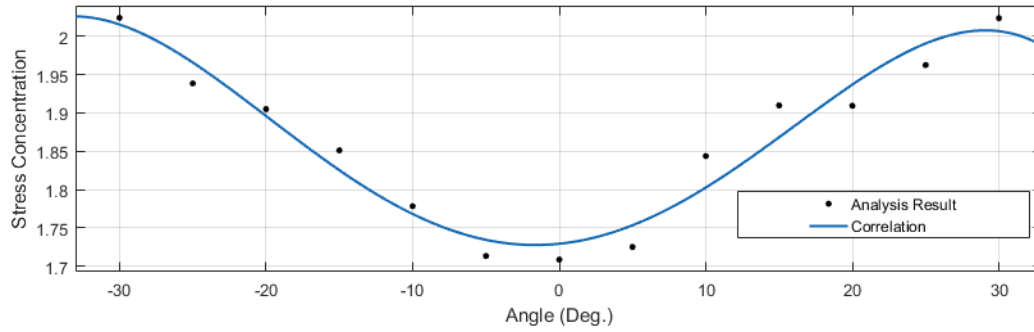


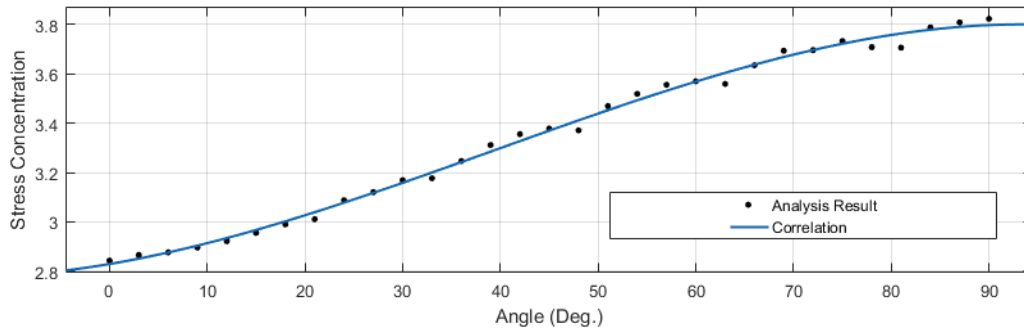
Fig 14. Von Mises stress contours ($\theta=30$ and $\varphi=0$), Bending Moment



Plot 11. Variation of Maximum Von Mises stress wrt. change in θ angle at $\phi=0$

From the above data it can be concluded that as the inclination of hole w.r.t. **Y-axis (in ZX Plane)** increases the Maximum Von Mises stress decreases. The correlation is accurate upto ± 30 deg.

4.1.2.3. Rotation in XY Plane with Z inclination of 30



Plot 12. Variation of Maximum Von Mises stress wrt. change in ϕ angle at $\theta=30$

From above data it can be concluded that as hole swivels from X-axis towards Y-axis in XY Plane the Maximum Von Mises stress increases. As shown in plot 12.

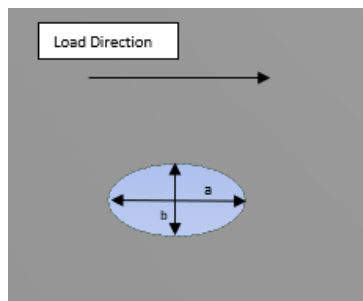


Fig 15. Elliptic Hole notations

4.2. Elliptic Hole

Elliptic hole was taken and the stresses were evaluated for different axes length and orientation.

a (b=8) in mm	Maximum Von-Mises	b (a=8) in mm	Maximum Von-Mises	a=10, b=5 φ (θ=0) in degrees	Maximum Von-Mises
5	3.775003272	5	2.254738862	0	2.018200436
6	3.503595351	6	2.47176813	5	2.042348973
7	3.157529609	7	2.705849763	10	2.115354484
8	2.986366086	8	2.986366086	15	2.235155993
9	2.699882714	9	3.131902933	20	2.427588366
10	2.611124237	10	3.341248922	25	2.56713079
11	2.502696789	11	3.670628077	30	2.747426438
12	2.366460299	12	3.841032556	35	3.021522059
13	2.282082672	13	4.207399095	40	3.049544543
14	2.182679618	14	4.623352057	45	3.499648603
15	2.112900316	15	4.39678849	50	3.645373702
		16	4.416272864	55	3.860222549
		17	4.977579151	60	3.916242421
		18	5.244415424	65	3.99144791
		19	5.5882146	70	4.147508461
		20	5.300802244	75	4.197422158
				80	4.174294017
				85	3.879648794
				90	4.204951909

Table 4. Stress concentration with hole axis dimensions and orientation

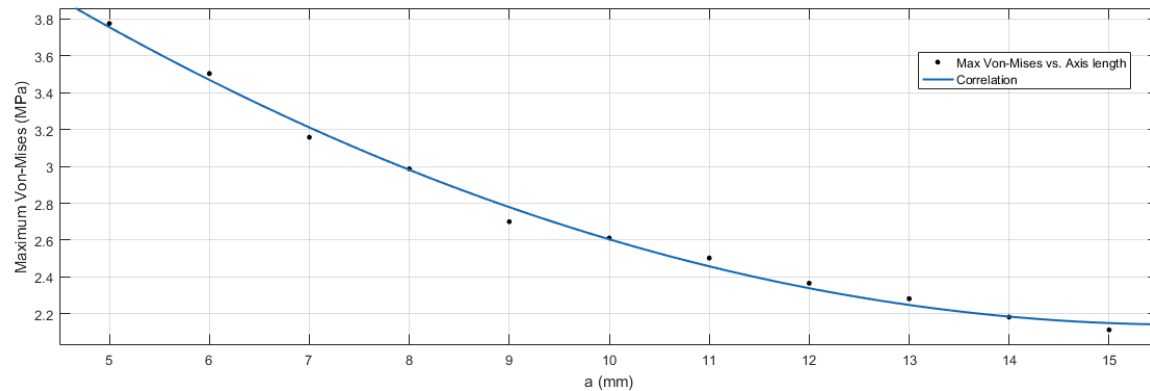
In case of elliptical hole maximum normal stress is given by,

$$\sigma_{max} = \sigma \left(1 + 2 \frac{b}{a} \right) \quad 18$$

Where **a** and **b** are semi major and semi minor axis respectively with semi minor axis aligned along the load axis.

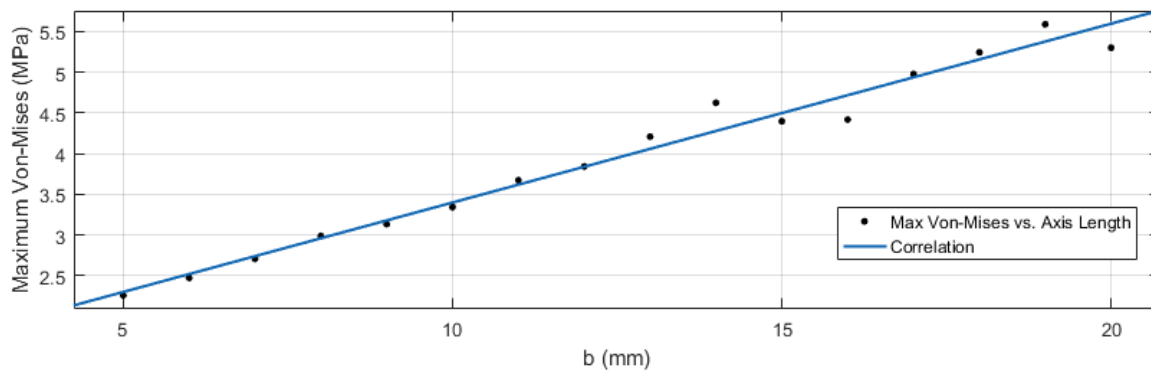
Results are in agreement with the equation 3.

4.2.1. Variation in axis length



Plot 13. Stress cocentration vs. a axis variation

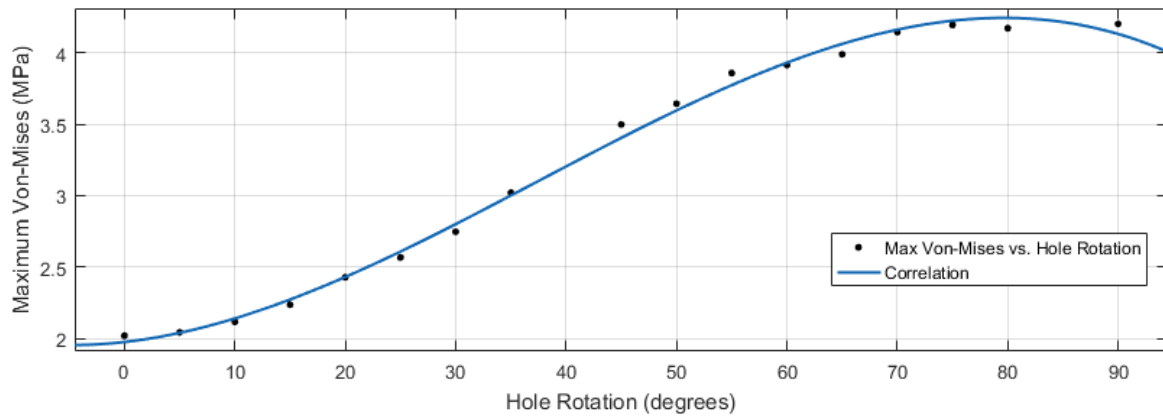
From the analysis results it can be seen that as the length of axis (a) lying along load axis increases, the stress cocentration decreases. As shown in plot.



Plot 14. Stress cocentration vs. b axis variation

From the analysis results it can be seen that as the length of axis (b) lying perpendicular to the load axis increases, the stress cocentration aslo increases. As shown in plot.

4.2.2. Variation in axis orientation



Plot 15. Stress concentration vs. hole orientation (φ)

From the analysis results it can be deduced that as the major axis is rotated from the load axis towards the transverse axis, the stress concentration also increases. As shown in plot.

Conclusion

The effect of inclination, size and orientation of hole (in a finite plate with finite thickness under uniaxial loading) on the stress concentration factor is studied. Also, the case of elliptic hole is considered. The results are obtained after doing analysis in Ansys Mechanical APDL and compared with the results obtained from the available equations for straight holes. The generated results are in accordance with the results obtained from the equations. Hence, alternatively, the finite element approach used in this study can be implemented for obtaining solutions for general cases having inclined holes without losing much accuracy.

References:

1. Theory of Elasticity -Timoshenko, pp. 78-83.
2. Effects of the Position and the Inclination of the Hole in Thin Plate on the Stress Concentration Factor. Mohammed Diany, Université Sultan Moulay Slimane, Faculté des Sciences et Techniques Béni Mellal, Morocco Laboratoire Génie Industrie.
3. The Finite Element Method and Applications in Engineering Using ANSYS –Erdogan Madenci, Ibrahim Guven.
4. Finite Element Analysis of Elastic Stresses around Holes in Plate Subjected to Uniform Tensile Loading. B. Mallikarjun, P. Dinesh, K.I. Parashivamurthy.

ORIGINALITY REPORT

19%

SIMILARITY INDEX

8%

INTERNET SOURCES

6%

PUBLICATIONS

18%

STUDENT PAPERS

PRIMARY SOURCES

1	Submitted to Institute of Technology, Nirma University Student Paper	5%
2	Submitted to University of Durham Student Paper	2%
3	Submitted to University of Sydney Student Paper	1%
4	cpx.endisinsight.com Internet Source	1%
5	Submitted to University of Bristol Student Paper	1%
6	Submitted to University of Leeds Student Paper	1%
7	Submitted to University of Glasgow Student Paper	1%
8	Submitted to University of Birmingham Student Paper	1%
9	www.math.ohiou.edu	
